A metal:p-n-CdTe Schottky-barrier solar cell: Photoelectrochemical generation of a shallow p-type region in n-CdTe

J. Richard Pugh, Duli Mao, Ji-Guang Zhang, Michael J. Heben, Arthur J. Nelson, and Arthur J. Frank[a]
National Renewable Energy Laboratory, 1617 Cole Boulevard, Golden, Colorado 80401

(Received 11 December 1992; accepted for publication 4 May 1993)

A simple method for producing a Au:*p-n*-CdTe Schottky barrier is described. The shallow *p-n* junction is formed by photoelectrochemical surface oxidization of *n*-CdTe. X-ray photoelectron spectroscopy, Auger electron spectroscopy depth profiling, and electron-beam-induced-current measurements provide important insight into the underlying causes of the formation of the *p*-type layer. Current-voltage and capacitance-voltage measurements show that the thin *p*-layer enhances the effective barrier height relative to that of a traditional Au:*n*-CdTe junction. These results account for the Au:*p-n*-CdTe cells exhibiting higher open-circuit photovoltages and higher photoconversion efficiencies than do Au:*n*-CdTe Schottky-barrier cells. From temperature dependence studies of the current-voltage characteristics, detailed information on the charge-transport mechanism of the junction was obtained. Photocurrent spectra of Au:*p-n*-CdTe as a function of temperature reveal that exciton excitation in CdTe contributes to the photocurrent.

I. INTRODUCTION

CdTe is of interest for thin-film photovoltaic devices because of its almost ideal band gap of 1.47 eV for optical to electrical energy conversion[1] and its short optical-absorption length. However, as is often the case with small-band-gap semiconductors, the Schottky-barrier height at the metal-CdTe interface is dominated by Fermi-level pinning,[2] which limits the open-circuit photovoltage and the energy conversion efficiency attainable with CdTe-based Schottky-barrier-type solar cells. Several strategies have been applied to augment the effective Schottky-barrier height and, hence, the open-circuit photovoltage of metal-semiconductor junctions. Most commonly, a metal-insulator-semiconductor (MIS) structure is formed by growing an insulating (usually an oxide) layer on the semiconductor surface.[3] Alternatively, the formation of a thin *p*-type layer between the metal and *n*-type semiconductor can also enhance the barrier height, as was originally shown for the Al-Si contact.[4,5] Thin *p*-type layers have been formed on the surface of *n*-CdTe by ion implantation[6] and heat-induced gold diffusion.[7] Both of these techniques require high processing temperatures that can cause degradation of the semiconductor charge-transport properties. It is therefore worthwhile to explore other methods for forming a thin *p*-type surface layer in order to improve the performance of CdTe-based solar cells.

A promising approach for forming a *p*-layer involves the photoelectrochemical oxidation of the *n*-CdTe surface. As with other narrow-band-gap *n*-type semiconductor electrodes,[8] CdTe is subject to photocorrosion in aqueous solution-based photoelectrochemical solar cells.[9,10] When illuminated with band-gap light, *n*-CdTe electrodes undergo solvent-assisted, multiple-valence-band hole oxidation of the surface. Degradation of the CdTe surface occurs according to

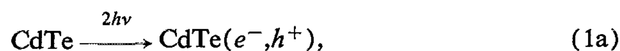

$$\mathrm{CdTe} \xrightarrow{2h\nu} \mathrm{CdTe}(e^-,h^+), \tag{1a}$$

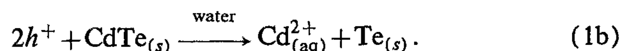

$$2h^+ + \mathrm{CdTe}_{(s)} \xrightarrow{\text{water}} \mathrm{Cd}^{2+}_{(\mathrm{aq})} + \mathrm{Te}_{(s)}. \tag{1b}$$

The out-diffusion of Cd^{2+} ions from the *n*-CdTe substrate leaves behind Cd vacancies that act as acceptors, creating a *p*-type surface layer.[11,12] With continued photoanodic dissolution, the short-circuit photocurrent, open-circuit photovoltage V_{oc}, and photoconversion efficiency of the *n*-CdTe aqueous electrolyte solar cell deteriorate, leading to device failure.[13]

In this article, we demonstrate that the photoelectrolytic route for forming a *p* layer can be exploited to fabricate a solid-state metal:*p-n*-CdTe Schottky-barrier solar cell that displays higher power conversion efficiency than a metal:*n*-CdTe solar cell. Surface analysis studies and electrical measurements of the surface-modified CdTe provide detailed information on the chemical nature of the surface and the charge-transport mechanism, respectively.

II. EXPERIMENT

(111)-oriented single-crystal *n*-CdTe (Eagle Picher) square plates were $0.6\times5\times5$ mm^3 with resistivities ranging from 0.26 to 0.61 Ω cm. Backside ohmic contacts were made to the Cd-rich face by in-diffusion of indium at 200 °C under a nitrogen atmosphere for 1 h. The crystals were mounted on copper blocks and the exposed edges of CdTe were insulated with Torr Seal epoxy. The Te-rich front face was mechanically polished with 6.0 μm diamond and then with 0.25 μm alumina, etched in $K_2Cr_2O_7$:H_2SO_4 solution (seven parts saturated aqueous $K_2Cr_2O_7$: to three parts concentrated H_2SO_4) for 20 s, rinsed with H_2O and methanol, and then dried under a stream of N_2.

---

[a]Author to whom correspondence should be addressed.

Downloaded 28 May 2009 to 131.183.220.186. Redistribution subject to AIP license or copyright; see http://jap.aip.org/jap/copyright.jsp

Tetrabutylammonium hexafluorophosphate ($TBAPF_6$; Aldrich) was recrystallized from dichloromethane and diethyl ether and dried under vacuum at 80 °C for 12 h prior to use. Spectrograde propylene carbonate (Burdick and Jackson) was used as received. The Te-rich face of *n*-CdTe was oxidized photoelectrochemically in a three-electrode one-compartment cell, consisting of an indium-tin oxide counterelectrode and a saturated calomel reference electrode (SCE). Solutions used for photoelectrochemical oxidation contained 0.1 M $TBAPF_6$ in propylene carbonate; these solutions were thermostated at 10 °C and deaerated by nitrogen bubbling. The applied potential was held at 2.0 V (versus SCE), and the intensity of light from a tungsten-halogen lamp, incident on the CdTe, was adjusted to maintain a current density of 1 mA cm^{-2}. The best photovoltaic behavior was obtained with electrodes in which about 0.08 C cm^{-2} had been passed. After photoelectrolysis, the CdTe electrodes were removed from solution, rinsed with methanol, and dried under a N_2 stream. Finally, a small gold contact pad was vacuum evaporated onto the CdTe surface. The junction area of the CdTe crystals exposed to light was typically 0.04–0.08 cm^2. The photoelectrochemically generated junction was compared with a standard CdTe Schottky-barrier device that was formed by depositing Au onto freshly etched CdTe.

Current-voltage (*J-V*) measurements were performed with a Princeton Applied Research Corp. (PAR) model 173 potentiostat and PAR model 175 universal programmer. For photovoltaic power-curve measurements, the incident radiant power from a 250 W quartz tungsten-halogen lamp (Oriel) was 100 mW cm^{-2}, as measured with an IL1700 radiometer (International Light, Inc.). Capacitance-voltage (*C-V*) measurements were made with a Brookdeal 9505SC lock-in amplifier, Hewlett-Packard 3325A frequency synthesizer, and PAR 173 potentiostat. Photoaction spectra were obtained with chopped monochromatic light referenced to a lock-in amplifier; the spectral data were normalized with respect to the lamp spectra. Data acquisition and reduction of *J-V*, *C-V*, and photoaction spectra were done by computer. Typically, a CdTe sample was mounted on a copper block and fixed in a cold finger of a closed-cycle helium cryostat (Air Products) for low-temperature measurements. The temperature of the sample was controlled by a silicon diode sensor and a Scientific Instruments model 9620-1 temperature controller.

X-ray photoelectron spectra (XPS) and Auger electron spectra (AES) were recorded on a Perkin-Elmer/Physical Electronics Model 550 ESCA system having a base pressure of 5×10^{-10} Torr. The data were acquired with Mg$K\alpha$ radiation ($h\nu=1253.6$ eV) and adjusted for differences in atomic sensitivity. Electron-beam-induced-current (EBIC) measurements were performed with a JEOL-JSM 840 scanning electron microscope (SEM).

III. RESULTS AND DISCUSSION

A. Surface characterization

X-ray photoelectron spectroscopy (XPS) revealed that the surface composition of *n*-CdTe underwent a major chemical transformation during photoelectrolysis. Figure 1(a) shows that before photoelectrolysis, a freshly etched CdTe crystal was covered with a Te-rich surface layer within a probe depth of 30–50 Å. The intensity of the Te 3*d* peak was 20 times that of the Cd 3*d* peak. Furthermore, the Te 3*d* line shape [inset of Fig. 1(a)] gives no evidence for the formation of tellurium oxide, indicating that the etchant (chromic acid) oxidizes Te^{2-} of CdTe to elemental (metallic) Te, in good agreement with published results.[14] However, it is important to point out that over time tellurium oxide did form as a result of the reaction of elemental tellurium with air. We found no indication of tellurium oxide when samples were kept under vacuum. A comparison of the spectra in Figs. 1(a) and 1(b) shows that after photoelectrolysis, the Te:Cd ratio declined from 20:1 to 3:1, implying that a significant fraction of the surface Te had dissolved into solution. Moreover, the Te 3*d* line shape [inset of Fig. 1(b)] shows the presence of the Te $3d_{5/2}$ peak at a binding energy of 575.8 eV, which is indicative of TeO_2. The Te $3d_{5/2}$ peak at 577 eV, corresponding to the thermodynamically more favorable TeO_3, was not detected. The low-energy Te $3d_{5/2}$ peak at 572.7 eV can be ascribed to either elemental Te or Te^{2-} of CdTe. In view of the relatively high intensity of the Cd 3*d* peak, the low-energy Te $3d_{5/2}$ is assigned predominantly to the presence of Te^{2-} of CdTe. Quantitative analysis of the Te 3*d* line shape indicates that 67% of the photoelectrons are due to Te in TeO_2 and the remainder are due to Te^{2-} of CdTe. In order to investigate a region closer to the surface, we employed low-angle XPS in which only photoelectrons emitted at a near-grazing angle to the surface were detected. The low-angle XPS spectrum revealed a

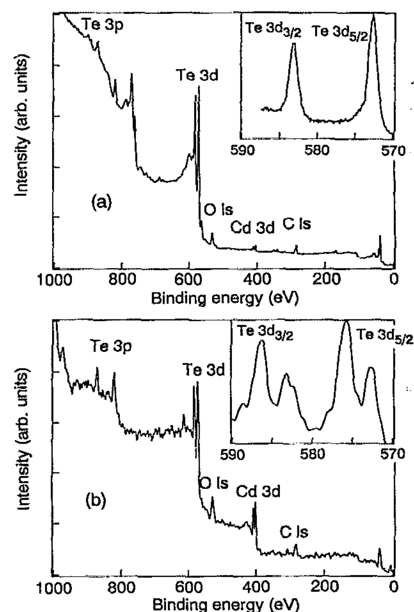

FIG. 1. X-ray photoelectron spectra of the (111) Te face of *n*-CdTe crystals (a) immediately after etching in $K_2Cr_2O_7$:H_2SO_4 and (b) after photoelectrochemical oxidation. Insets are expanded spectra of the Te 3*d* region.

Downloaded 28 May 2009 to 131.183.220.186. Redistribution subject to AIP license or copyright; see http://jap.aip.org/jap/copyright.jsp

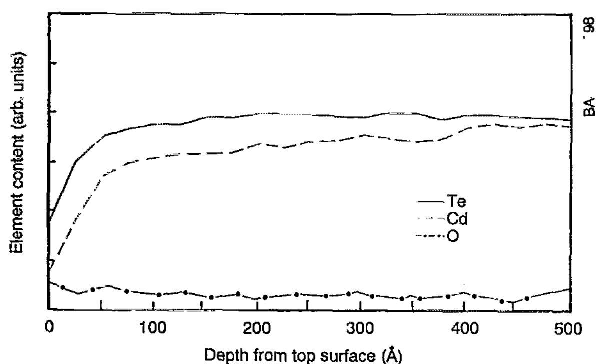

FIG. 2. Auger depth profile of a photoelectrochemically treated n-CdTe sample.

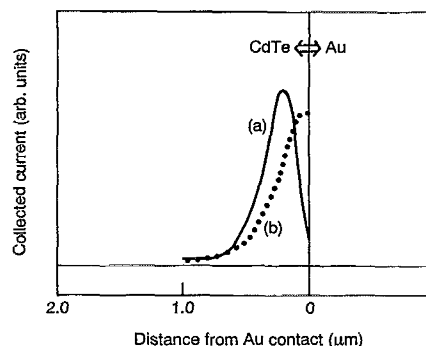

FIG. 3. EBIC measurements of CdTe crystals overlaid with a gold film deposit. Cross-sectional scan of freshly cleaved CdTe face normal to the gold contact: (a) photoelectrochemically treated n-CdTe; (b) untreated n-CdTe.

Te:Cd ratio of 4.5:1, which is higher than the 3:1 ratio obtained from the relatively bulk-sensitive integrated XPS spectrum, suggesting that the outermost surface layer is dominated by TeO_2 and that the observed Cd signal originates mainly from the subsurface region. More specifically, these results imply that photoelectrolysis produces a thin TeO_2 overlayer (20–30 Å) on the bulk CdTe.

To determine the stoichiometry of the near-surface region of CdTe, Auger-depth-profile studies were made. Figure 2 displays the elemental profile perpendicular to the surface when the rate of Ar-ion-beam sputtering is 48 ± 10 Å min^{-1}. The oxygen (KVV) signal disappears within 30 Å of the surface, implying that the TeO_2 layer is very thin. The Te (MNN) signal rises rapidly within the first 30 Å, reaching a constant level at about 180 Å below the surface. Significantly, the intensity of the Cd (MNN) signal is considerably below that of Te for a depth of 450 Å, suggesting a Cd-deficient layer of comparable thickness. The nonstoichiometric surface implies that a high density of Cd vacancies is generated in the near-surface region by photoelectrolysis. Taking into consideration the acceptor nature of Cd vacancies in CdTe,[11,12] the depth-profile result provides strong evidence for the formation of a p-type region near the surface of CdTe. It is worthwhile to note that a large nonstoichiometry does not necessarily reflect a high concentration of hole carriers near the CdTe surface because, as ion implantation studies have shown,[6] only a small fraction of the Cd vacancies may be electrically active.

B. Electron-beam-induced current (EBIC)

Direct evidence for the presence of a p-type layer at the surface of photoelectrolytically treated CdTe comes from EBIC studies. Figure 3 displays data for both the surface-treated CdTe electrode and the Au:n-CdTe Schottky-barrier diode. In either case, a gold overlayer was deposited onto the front face of CdTe crystals for electrical contact, and the crystals were cleaved along the (100) direction to generate a fresh cross section just prior to measurements. Low-electron-beam energies, from 2 to 5 keV, were employed in these EBIC measurements for high resolution, albeit at some sacrifice of the resolution of the SEM imaging of the gold-semiconductor interface. In Fig. 3(a), the EBIC profile of the photoelectrolytically treated CdTe shows clearly the presence of a p-n junction buried 250 nm beneath the surface of CdTe. For comparison, Fig. 3(b) shows a cross-sectional scan of a freshly cleaved Au:n-CdTe Schottky-barrier diode. The Au:n-CdTe data are in good agreement with published results.[7] Taking into consideration that the electron beam (2 keV) corresponds to an electron range of 56 nm, the EBIC profile indicates that gold does not diffuse significantly into the CdTe at room temperature, and that CdTe remains n type even near the Au:CdTe metallurgical interface. Thus, the formation of the p region cannot be attributed to the diffusion of gold into the CdTe but must be related to the photoanodic oxidation of the surface.

C. Current-voltage behavior

The dark J-V characteristics of the Au:p-n-CdTe cell are rectifying. If the thermionic emission model for a Schottky barrier is assumed, the dependence of the current density J and the applied bias V_b can be expressed by[15]

$$J = J_0 \exp(qV_b/nkT), \tag{2}$$

where J_0 is the saturation current density, q is the electronic charge, n is the ideality factor, k is the Boltzmann constant, and T is the absolute temperature. The Schottky-barrier height Φ_B is deduced from J_0 by using the Richardson equation,

$$J_0 = A^* T^2 \exp(-q\Phi_b/kT), \tag{3}$$

where $A^* = A(m^*/m_e)$, $m^* = 0.1m_e$ is the effective electron mass for n-CdTe,[16] and $A = 120$ A cm^{-2} K^{-2} is the Richardson constant for free electrons.

Figure 4 shows a linear relationship between log J and the forward applied bias V_b between 0.35 and 0.65 V. Analysis of the plot, with the aid of Eqs. (2) and (3), gives a barrier height Φ_B of 1.05 eV and an ideality factor n of 1.33. The barrier heights of metal:n-CdTe contacts extend over a relatively wide range of values. Most metals, including gold, when deposited onto the surface of n-CdTe yield a Schottky-barrier height of about 0.72 eV. However, for

Downloaded 28 May 2009 to 131.183.220.186. Redistribution subject to AIP license or copyright; see http://jap.aip.org/jap/copyright.jsp

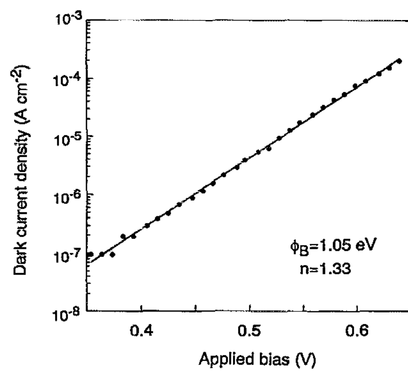

FIG. 4. Logarithmic dependence of the dark current at forward applied bias for Au:p-n-CdTe. n-CdTe oxidized by passing 0.076 C cm^{-2}.

reasons not well understood, deposition of gold on stoichiometric,[17] Cd-rich,[18] or Au-Cd alloyed[19] CdTe surfaces has also produced barrier heights as high as 0.93 eV. In general, the barrier heights measured for Au:p-n-CdTe were consistently higher than the ones that we and others[17–19] have determined for Au:n-CdTe.

Figure 5 shows the photovoltaic response of Au:p-n-CdTe. Under illumination with polychromatic light of 100 mW cm^{-2} intensity, the cell had a V_{oc} of 0.49 V, a short-circuit photocurrent J_{sc} of 4.9 mA cm^{-2}, a fill factor (FF) of 0.5, and a photoconversion efficiency of 1.2%. For comparison, when the light intensity was adjusted to yield the same J_{sc} value (4.9 mA cm^{-2}), a Au:n-CdTe device produced a V_{oc} of 0.32 V and a FF of 0.51. From measurements of different Au:p-n-CdTe cells, the following maximum values of individual parameters were obtained: V_{oc}=0.56 V, J_{sc}=7 mA cm^{-2}, and FF=0.72, suggesting that further improvement in the energy-conversion efficiency is achievable.

The experimental V_{oc} can be compared with the bulk-recombination-limited value V_{oc}^{max} using the expression[20]

$$V_{oc}^{max}=kT/q \ln[(J_{sc}L_pN_D)/qn_i^2D_p], \qquad (4)$$

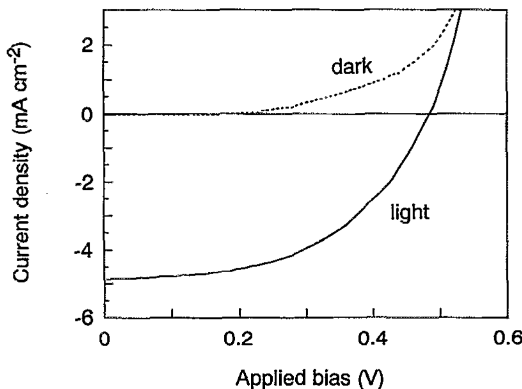

FIG. 5. Light (solid line) and dark (dotted line) current-voltage characteristics of Au:p-n-CdTe with a junction area of 0.08 cm^2. Incident radiant power was 100 mW cm^{-2} (tungsten-halogen lamp).

where L_p is the minority-carrier diffusion length, N_D is the doping concentration, and D_p is the diffusivity. The doping concentration N_D was determined to be 5×10^{15} cm^{-3} from C-V data discussed below. The diffusivity was calculated from the relation $D_p=\mu kT/q$, where the hole mobility μ in CdTe was taken to be 40 cm^2 V^{-1} s^{-1}.[21] The minority-carrier diffusion length was evaluated with the expression $L_p=(D_p\tau)^{1/2}$, using a minority-carrier lifetime of 3 ns, which was determined from a photoluminescence measurement. The intrinsic carrier concentration n_i was taken as 6.9×10^5 cm^{-3}.[21] Substituting the numerical values into Eq. (4), a maximum open-circuit photovoltage V_{oc}^{max} of 0.97 V was obtained, assuming a J_{sc} of 2 mA cm^{-2}. Thus, the theoretical V_{oc}^{max} (0.97 V) is 40% higher than the experimental values, indicating that the Au:p-n-CdTe cell is not bulk-recombination limited. Further improvements in the performance of the cell can be achieved by optimizing the conditions for photoanodic oxidation of the n-CdTe surface.

Current-voltage measurements of the photoelectrolytically modified n-CdTe surface yielded further evidence for the presence of a buried p-type layer. Illumination of the junction in which the gold electrical contact was masked off from the light produced about 60% of the photocurrent of the junction in which the gold contact was exposed to the light. Since the diffusion length of the minority carrier is less than 1 μm in the CdTe layer, as deduced from EBIC measurements, we infer that the surface modification produces a shallow homojunction that collects photocurrent from areas beyond the Au electrode contact. Thus, the shallow p-layer has relatively low surface resistivity and serves as a hole-conduction pathway to the gold contact. A similar approach has been utilized to improve charge transport in MIS photovoltaic solar cells.[22]

In order to gain insight into the nature of the charge-transport mechanisms of the Au:p-n-CdTe junction, the temperature dependence of the forward dark J-V characteristics were investigated. Figure 6 shows a linear relationship between $\log J$ and the forward applied bias V_b over more than two orders of magnitude in the temperature range of 220–380 K. At high forward bias, a negative deviation from linearity is observed that is ascribed to series resistance. At low bias, the positive departure from linearity can be traced to space-charge recombination. Extrapolation of the linear portion of the curves to zero applied bias gives the saturation-current density J_0 [via Eq. (3)], which is plotted as a function of temperature in Fig. 7. From the temperature dependence of J_0 the activation energy for current transport can be assessed. In the upper temperature range above 300 K the activation energy is 0.92 eV. This activation energy is identical to the value for the Schottky-barrier height deduced from the thermionic emission equation for this particular diode and indicates that thermionic emission is the dominant charge-transport mechanism at room temperature and above. The intercept of the line with the $\log(J_0/T^2)$ axis yields an effective Richardson constant of 16, in good agreement with the theoretical value.[12] The concurrence of the experimental and theoretical values provides further support for the use of

Downloaded 28 May 2009 to 131.183.220.186. Redistribution subject to AIP license or copyright; see http://jap.aip.org/jap/copyright.jsp

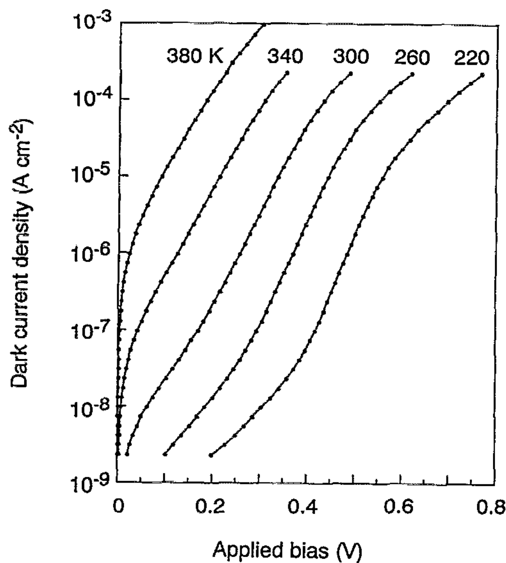

FIG. 6. Dark current-voltage curves for Au:p-n-CdTe at various temperatures.

the Schottky-barrier equation in analyzing the J-V data. The p-type layer is sufficiently thin that it merely enhances the barrier height of the metal:semiconductor Schottky junction, as was first demonstrated for the Al:n-Si Schottky diode.[4,5] At low temperatures the diode shows an activation energy of 0.68 eV, which is close to half of the band gap of CdTe, indicating that carrier recombination in the depletion layer plays a role below 300 K. At low temperatures, space-charge recombination is expected to be predominant in Schottky diodes with high barriers.

Figure 8 displays the temperature dependence of the ideality factor as determined from the data in Fig. 7 and Eq. (2). Above a temperature of 290 K, the ideality factor n declines slowly from a value of 1.4. The deviation from the ideal value of $n=1$ shows that current transport in the buried p-n Schottky diode departs from the ideal thermionic emission theory. Below a temperature of 290 K, the ideality factor increases steadily as the temperature decreases, reaching a value of about 2 at 100 K. This result

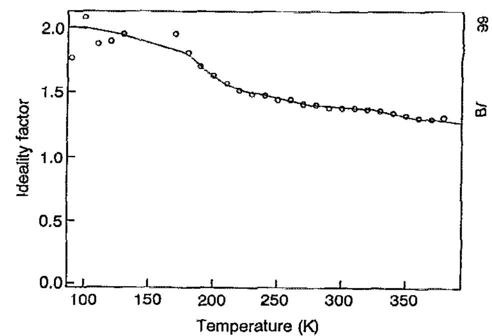

FIG. 8. Temperature dependence of the ideality factor of Au:p-n-CdTe.

indicates that space-charge recombination becomes increasingly important at lower temperatures, consistent with the analysis of $\log(J_0/T^2)$. At temperatures below 75 K (not shown in the figure), ideality factors much greater than 2 were obtained, in contrast to a plot of nkT vs T^{-1}, which was independent of temperature. The invariance of nkT with T^{-1} is characteristic of a tunneling mechanism[23] and implies that electron tunneling through the Schottky barrier is the principal current-transport mechanism at temperatures below 75 K.

Several groups have reported the presence of shallow p-regions at n-CdTe surfaces formed by ion implantation.[6] The J-V characteristics of these junctions invariably show ideality factors close to 2 at room temperature, indicating the presence of a high density of recombination centers in the near-surface region. In contrast, the data presented in our study demonstrate that the room-temperature charge transport is dominated by thermionic emission, implying that the electrochemical method produces a more defect-free p-type region than the ion implantation method.

D. Capacitance-voltage behavior

Figure 9 shows that the dark C-V data of Au:p-n-CdTe and Au:n-CdTe junctions display good Mott–Schottky behavior. The barrier height Φ_B was determined from the C^{-2} vs V plot with the expressions[15]

$$q\Phi_B = qV_{bi} + kT\ln(N_c/N_d) + kT, \qquad (5)$$

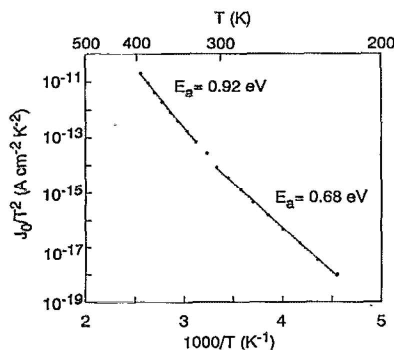

FIG. 7. Temperature dependence of J_0/T^{-2} (J_0 is the saturation current) of Au:p-n-CdTe.

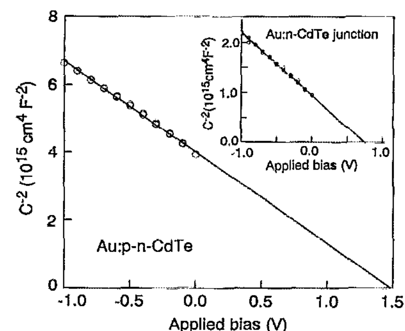

FIG. 9. Mott–Schottky plot of the same Au:p-n-CdTe sample used for J-V measurements in Fig. 4. Inset shows a Mott–Schottky plot of Au:n-CdTe. Modulation frequency was 1 kHz.

Downloaded 28 May 2009 to 131.183.220.186. Redistribution subject to AIP license or copyright; see http://jap.aip.org/jap/copyright.jsp

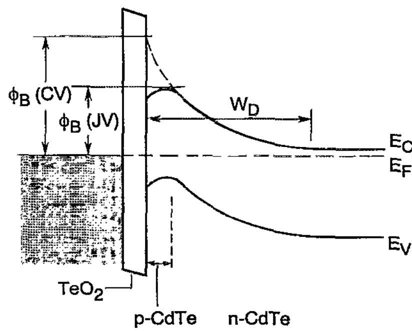

FIG. 10. Energy-band diagram of the Au:p-n-CdTe junction.

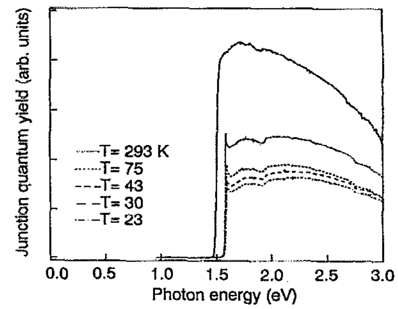

FIG. 11. Temperature dependence of photocurrent spectra of a Au:p-n-CdTe junction at zero applied bias.

$$N_d = -\left(\frac{2}{q\epsilon_0\epsilon_s}\right)\left(\frac{dC^{-2}}{dV}\right)^{-1}, \tag{6}$$

where the built-in voltage (band bending) V_{bi} is the intercept of the voltage axis, N_d is the majority-carrier concentration, N_c is the effective density of states in the conduction band, and ϵ_0 is the permittivity in vacuum. The built-in voltage V_{bi} of Au:p-n-CdTe is seen from the plot to equal 1.48 V. The static dielectric constant ϵ_s of CdTe was taken to be 11.[16] The effective density of states N_c of n-CdTe was calculated with the aid of the usual expression[15] to be 1.3×10^{18} cm^{-3}. The carrier concentration N_d was calculated to be 5×10^{15} cm^{-3}. Substituting these numerical values into Eq. (5) gives a barrier height of 1.64 eV. For comparison, the data for the Au:n-CdTe junction (insert of Fig. 9) yield a barrier height of 0.91 eV, about 0.7 eV less than the barrier height of the Au:p-n-CdTe junction. Both V_{bi} (1.48 V) and Φ_B (1.64 eV) of the Au:p-n-CdTe junction are, however, anomalously high in relation to the magnitude of the bandgap (1.47 eV). The basis for this phenomenon can be understood from the simplified energy-band diagram of a Au:p-n-CdTe junction depicted in Fig. 10. This diagram accounts for the observation that C-V measurements yield a higher barrier height (Φ_B=1.64 eV) than J-V measurements (Φ_B=1.05 eV). With the C-V technique, the barrier height is not measured directly but is inferred from a measurement of the reverse-bias characteristics of the interface. The Mott–Schottky analysis assumes that the barrier height increases parabolically toward the metal. If the barrier is nonparabolic for some reason, such as due to the presence of a shallow p region between n-type CdTe and the gold overlayer, the Mott–Schottky analysis will overestimate the barrier height and the built-in voltage. Thus, the J-V characteristics of the junction provide a more realistic measure of the barrier height than do the C-V data. However, the C-V data give further evidence for the presence of a thin p-type layer at the Au:CdTe interface.

The occurrence of an energy-barrier maximum at a distance beneath the metal contact causes a barrier height dependence on the applied bias.[23,24] This bias dependence, along with space-charge recombination and other effects, can contribute to the deviation of the ideality factor from unity and can lead to an underestimation of the barrier height. Modifications to the Richardson equation have been made for calculating a more accurate barrier height in the presence of space-charge recombination from J-V data.[25] Using these expressions and the values for the apparent barrier height and ideality factor deduced from J-V data (Fig. 4), we obtained a barrier height of 1.36 eV, which is 0.28 eV smaller than the barrier height determined from C-V data. This discrepancy supports the notion that the nonideality of the Au:p-n-CdTe contact arises, in part, from the bias dependence of the barrier height.

E. Photocurrent spectroscopy

Figure 11 illustrates the photoaction spectra (quantum yield versus wavelength or photon energy) of a representative junction under zero applied bias at several temperatures. At room temperature the pronounced rise in the photocurrent at 835 nm (1.48 eV) corresponds to the onset of the band-gap absorption of CdTe. The quantum yield passes through a maximum between 830 and 600 nm and then drops off with decreasing wavelengths ($\lambda<600$ nm). Comparison with the photoaction spectrum of a Au:n-CdTe sample (not shown in the figure) shows no difference from the spectral response of the Au:p-n-CdTe junction, indicating that no significant degradation in charge-transport properties occurs during the photoelectrolysis process. As the temperature of the Au:p-n-CdTe junction decreases, several features are evident in the spectra. The onset of the photocurrent increases from 1.48 eV at room temperature to 1.57 eV at 75 K. Further decrease of the temperature produces only a negligible shift in the photocurrent onset to higher photon energies. This shift in photocurrent onset is consistent with the temperature dependence of the band gap of CdTe[21] and can be correlated with entropic effects in the formation of charge carriers.[26] The presence of a sharp peak near the onset of the photoaction spectra below room temperature suggests that the steep rise in photocurrent is not only associated with the direct band-to-band electronic transition of CdTe but also with exciton excitation in the semiconductor. Finally, the decline in quantum efficiency at low temperatures is due to an increase in the series resistance of the junction.

Downloaded 28 May 2009 to 131.183.220.186. Redistribution subject to AIP license or copyright; see http://jap.aip.org/jap/copyright.jsp

IV. CONCLUSION

The photoelectrochemical oxidation of *n*-CdTe leads to the formation of a thin TeO_2 layer at the surface of the semiconductor. Depletion of Cd from the near-surface region of *n*-CdTe during photoelectrolysis leaves behind Cd vacancies, resulting in a thin *p*-type region between the oxide layer and the bulk *n*-CdTe. The subsequent deposition of a gold film on the photoelectrolytically treated CdTe leads to a Au:*p*-*n*-CdTe structure that behaves as a modified Schottky-barrier device. The thin *p*-type layer increases the effective Schottky-barrier height and improves the performance of the solar cell. The ability to induce a shallow *p*-type region in *n*-CdTe at room temperature by photoelectrolysis offers a new and useful alternative to ion-implantation and gold-diffusion techniques for improving the efficiency of CdTe-based Schottky-barrier solar cells.

ACKNOWLEDGMENTS

We are grateful to Richard Matson for EBIC measurements and to Amy Swartzlander-Franz for Auger electron spectroscopy measurements. This work was supported by the Office of Basic Energy Sciences, Division of Chemical Sciences, U.S. Department of Energy, under Contract No. DE-AC02-83CH10093.

[1] J. J. Lofersky, J. Appl. Phys. **27**, 777 (1956).
[2] I. M. Dharmadasa, A. B. McLean, M. H. Patterson, and R. H. Williams, Semicond. Sci. Technol. **2**, 404 (1987).
[3] J. G. Werthen, J.-P. Häring, and R. H. Bube, J. Appl. Phys. **54**, 1159 (1983).
[4] J. M. Shannon, Solid-State Electron. **19**, 537 (1976).
[5] K. Chino, Solid-State Electron. **16**, 119 (1973).
[6] M. Chu, A. L. Fahrenbruch, R. H. Bube, and J. F. Gibbons, J. Appl. Phys. **49**, 322 (1978), and references therein.
[7] P. Gaugash and A. G. Milnes, J. Electrochem. Soc. **128**, 921 (1981).
[8] R. Noufi, A. J. Frank, and A. J. Nozik, J. Am. Chem. Soc. **103**, 1849 (1981); F. F.-R Fan, B. L. Wheeler, A. J. Bard, and R. Noufi, J. Electrochem. Soc. **128**, 2042 (1981); R. A. Simon, R. A. Ricco, and M. S. Wrighton, J. Am. Chem. Soc. **104**, 2031 (1982); G. Horowitz, G. Tourillon, and F. Garnier, J. Electrochem. Soc. **131**, 151 (1984); A. J. Frank, S. Glenis, and A. J. Nelson, J. Phys. Chem. **93**, 3818 (1989), and references therein.
[9] H. Gerischer and W. Mindt, Electrochim. Acta **13**, 1239 (1968).
[10] P. P. Konorov and S. M. Repinskii, Elektrokhimiya **4**, 226 (1968).
[11] C. Vázquez-López, F. Sánchez-Sinencio, J. S. Helman, J. L. Peña, A. Lastras-Martínez, P. M. Raccah, and R. Triboulet, J. Appl. Phys. **50**, 5391 (1979).
[12] X. I. Saldaña, C. Vázquez-López, A. Zehe, H. Navarro, and R. Triboulet, Appl. Phys. Lett. **39**, 433 (1981).
[13] A. B. Ellis, S. W. Kaiser, and M. S. Wrighton, J. Am. Chem. Soc. **98**, 6418 (1976).
[14] M. H. Patterson and R. H. Williams, J. Phys. D **11**, L83 (1978).
[15] S. M. Sze, *Physics of Semiconductor Devices* (Wiley, New York, 1981).
[16] K. Zanio, *Semiconductors and Semimetals: Cadmium Telluride* (Academic, New York, 1978), Vol. 13
[17] R. L. Van Meirhaeghe, R. Van der Walle, W. H. Laflére, and F. Cardon, J. Appl. Phys. **70**, 2200 (1991).
[18] I. M. Dharmadasa, J. M. Thornton, and R. H. Williams, Appl. Phys. Lett. **54**, 137 (1989).
[19] C. F. Keuch, J. Appl. Phys. **52**, 4874 (1981).
[20] N. S. Lewis, J. Electrochem. Soc. **131**, 2496 (1984).
[21] A. J. Strauss, Rev. Phys. Appl. **12**, 167 (1977).
[22] P. Van Halen, R. E. Thomas, R. Mertens, and R. Van Overstraeten, in *Proceedings of the 12th IEEE Photovoltaic Specialists' Conference*, Nov. 1976, Baton Rouge, LA (IEEE, New York, 1976), p. 907.
[23] E. H. Rhoderick and R. H. Williams, *Metal-Semiconductor Contacts* (Clarendon, Oxford, 1988).
[24] L. F. Wagner, R. W. Young, and A. Sugerman, IEEE Electron Device Lett. **EDL-4**, 320 (1983).
[25] A. B. McLean, I. M. Dharmadasa, and R. H. Williams, Semicond. Sci. Technol. **1**, 137 (1986).
[26] C. D. Thurmond, J. Electrochem. Soc. **122**, 1133 (1975).

Downloaded 28 May 2009 to 131.183.220.186. Redistribution subject to AIP license or copyright; see http://jap.aip.org/jap/copyright.jsp